J|A|C|S ARTICLES

Published on Web 04/08/2010

Solution and Solid-State Studies of Doubly Trimethylene-Bridged Tetraalkyl *p*-Phenylenediamine Diradical Dication Conformations

Almaz S. Jalilov,[†] Gaoquan Li,[†] Stephen F. Nelsen,*[,†] Ilia A. Guzei,[†,‡] and Qin Wu[§]

Department of Chemistry, University of Wisconsin, Madison, 1101 University Avenue, Madison, Wisconsin 53706-1396, and Molecular Structure Laboratory and Center for Functional Nanomaterials, Brookhaven National Laboratory, Upton, New York 11973

Received January 21, 2010; E-mail: nelsen@chem.wisc.edu

Abstract: X-ray crystallographic structures are reported for **1(Me)**$^{2+}$($SbCl_6^-$)$_2$·$2CH_3CN$, **2(Et)**$^{2+}$(SbF_6^-)$_2$·$2CH_3CN$·$2CH_2Cl_2$, and **1(iPr)**$^{2+}$(SbF_6^-)$_2$, which also contained unresolved solvent and is in a completely different conformation than the methyl- and ethyl-substituted compounds. A quite different structure of **1(Me)**$^{2+}$(SbF_6^-)$_2$ than that previously published was obtained upon crystallizing it from a mixture rich in monocation. It does not contain close intramolecular **PD**$^+$,**PD**$^+$ contacts but has close intermolecular ones. Low temperature NMR spectra of **1(Me)**$^{2+}$ and **1(Et)**$^{2+}$ in 2:1 CD_3OD/CD_3CN showed that both contain three conformations of all-gauche NCCC unit material with close intramolecular **PD**$^+$,**PD**$^+$ contacts. In addition to the both **PD**$^+$ ring *syn* and *anti* material that had been seen in the crystal structure of **1(Me)**$^{2+}$(SbF_6^-)$_2$·$2CH_3CN$ published previously, an unsymmetrical conformation having one **PD**$^+$ ring *syn* and the other *anti* (abbreviated *uns*) was seen, and the relative amounts of these conformations were significantly different for **1(Me)**$^{2+}$ and **1(Et)**$^{2+}$. Calculations that correctly obtain the relative amounts of both the methyl- and ethyl-substituted material as well as changes in the optical spectra between **1(Me)**$^{2+}$ and **1(Et)**$^{2+}$, which contains much less of the *uns* conformation, are reported.

Introduction

We recently reported a communication focused upon oxidation studies of the doubly trimethylene-bridged tetraaza[5,5]-*p*-phenylene diamine-(**PD**) containing paracyclophanes **1(R)**, R = methyl, ethyl, and isopropyl.[1] Neutral **1(Me)** is in the all-*anti* NCCC twist angle conformation drawn (which we will abbreviate as an *aa*,*aa* conformation), which keeps the **PD**^{0} rings as far apart as possible, in crystals as well as in the gas phase, where it is calculated to be the most stable conformation. However, the dication **1(Me)**$^{2+}$ is in *gg*,*gg* conformations that force π-stacking in crystals. The X-ray structure published contained both dications having both **PD**$^+$ units with their methyl groups *anti*, as well as dications in which both were *syn*. This conformational change in the trimethylene bridges leads to an unexpected redox inversion, in which the second electron is removed more easily than the first in the presence of supporting electrolyte. Although the behavior of **1(Et)** upon electron removal is very similar to that of **1(Me)**, **1(iPr)** behaves quite differently, with the second electron being 0.29 V (6.7 kcal/mol) harder to remove than the first. Its neutral form is in a *ga*,*ga* conformation, presumably because it is forced out of the *aa*,*aa* conformation by the presence of the branched alkyl groups. The optical spectra of **1(Me)**$^{2+}$ and **1(Et)**$^{2+}$ were shown to be very similar, but that of **1(iPr)**$^{2+}$ is quite different. This paper reports X-ray crystallographic studies of **1(R)**$^{2+}$ that establish their conformations in the solid state, NMR studies that elucidate the conformations present for **1(Me)**$^{2+}$ and **1(Et)**$^{2+}$, and calculations that assign the optical spectra of these compounds.

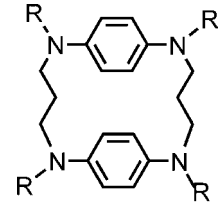

1(R)

Results

The X-ray crystallographic and proton NMR data will be discussed in that order. Two additional crystal structures of the methyl compound, one with a different counterion (**1(Me)**$^{2+}$($SbCl_6^-$)$_2$·$2CH_3CN$) and one with the dication unit in a different conformation than that previously reported (**1(Me)**$^{2+}$(SbF_6^-)$_2$ (including unresolved solvent)) are summarized in Table 1. Another structure in these series was also determined, that of **1(Me)**$^{2+}$(SbF_6^-)$_2$·$2(ClCH_2)_2$, but it has both *anti*,*anti* and *syn*,*syn* **1(Me)**$^{2+}$ units present, is badly disordered at the counterions, and is of low precision, so it will not be reported here. The structure of **1(Et)**$^{2+}$($SbCl_6^-$)$_2$·$2(CH_3CN)$·$2(CH_2Cl_2)$, which is very similar to that of solvated **1(Me)**$^{2+}$($SbCl_6^-$)$_2$, is also reported in Table 1. None of these structures have intermolecular close contacts between **1(R)**$^{2+}$ units, and all have **PD**$^+$ separations that are significantly less

[†] University of Wisconsin.
[‡] Molecular Structure Laboratory, University of Wisconsin.
[§] Center for Functional Nanomaterials, Brookhaven National Laboratory.

(1) Nelsen, S. F.; Li, G.; Schultz, K. P.; Guzei, I. A.; Tran, H. Q.; Evans, D. A. *J. Am. Chem. Soc.* **2008**, *130*, 11620–11622.

10.1021/ja100322k

Table 1. Comparison of **1(R)**$^{2+}$ X-ray Structures Having Intramolecular π-Stacking

compd	**1(Me)**$^{2+}$$(SbF_6^-)_2\cdot 2CH_3CN$[a] *anti*	**1(Me)**$^{2+}$$(SbCl_6^-)_2\cdot 2CH_3CN$[b] *anti*	**1(Et)**$^{2+}$$(SbCl_6^-)_2\cdot 2(CH_3CN)\cdot 2(CH_2Cl_2)$
NCCC conformations	*gg*,*gg*	*gg*,*gg*	*gg*,*gg*
PD$^+$ conformations	*anti*,*anti*	*anti*,*anti*	*anti*,*anti*
NCCC twists, deg	±67.2, ±65.2	±64.0, ±66.3	±63.2, ±62.2
d(N,N), Å	2.937(2)	2.929(9)	2.839(9)[e]
$d(C_q,C_q)$, Å	3.084(2)	3.062(9)[d]	3.01(1)[d]
smaller *d*(CH,CH), Å	3.156(3), 3.176(3)	3.131(1), 3.179(1)	3.14(1), 3.06(1)[e]
d(intra mean C_6 planes), Å	3.072	3.030	3.295
closest intermol *d*(CH,CH), Å	4.212(× 2)	3.943(× 2)	3.325,3.326
NC twists,[c] deg	±17.5, ±18.5, ±9.7, ±6.3	±22.0, ±16.3, ±0.8, ±7.6	±8.2, ±15.3, ±13.7, ±11.7

[a] From ref 1. Unit cell also contains the **PD**$^+$ *syn*,*syn* conformation but was modeled with same C_6 ring positions, so the *syn*,*syn* structure is not very good. [b] The unit cell was not modeled as containing the **PD**$^+$ *syn*,*syn* conformation, but its C_6 elipsoids are rather long. [c] C═C−N−R twist, C═C′−N−CH_2 twist; average is N(lp),C(p) twist. [d] Distance between pairs of quaternary ring carbons. [e] Statistically significantly smaller than for **1(Me)**$^{2+}$.

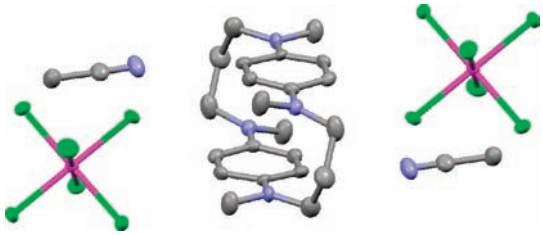

Figure 1. Crystal structure of **1(Me)**$^{2+}(SbCl_6^-)_2\cdot 2CH_3CN$.

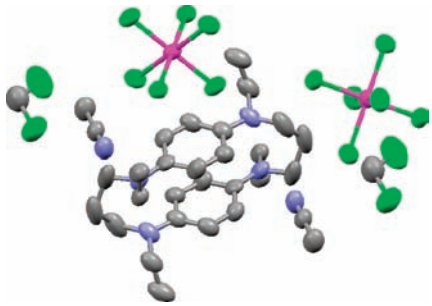

Figure 2. Crystal structure of **1(Et)**$^{2+}(SbCl_6^-)_2\cdot 2CH_3CN\cdot 2CH_2Cl_2$ with hydrogens omitted for clarity.

than van der Waals (vdW) contacts. The **1(Me)**$^{2+}$ structure with $SbCl_6^-$ counterions and two acetonitriles of solvation that is reported here (see Figure 1) is quite similar to that with SbF_6^- counterions and the same solvent in the crystal that was reported earlier,[1] although a *syn*,*syn* dication structure was not found in its crystal. The $SbCl_6$ anion is disordered over two positions with a minor component contribution of 16.5(12)%, and the errors are larger than for the SbF_6^- structure. The structure of the dication unit of **1(Et)**$^{2+}$ (Figure 2) is very similar to that of **1(Me)**$^{2+}$. More solvent fills in the spaces left by the ethyl instead of methyl groups, and the **PD**$^+$ units are slightly closer (see below).

A very different type of a **1(Me)**$^{2+}$ unit was obtained in an attempt to isolate the monocation, when crystals were grown from a solution having a large excess of neutral **1(Me)**. Although it has an NCCC *gg*,*gg* and **PD**$^+$ *syn*,*syn* structure, it is unrelated to the **PD**$^+$ *syn*,*syn* structure present in the published structure[1] because its **PD**$^+$ rings are displaced from each other instead of being held in position enforcing π-stacking; the signs of the NCCC twist angles are the same, instead of being opposite as they are in the π-stacked structure, see Figure 3. We will abbreviate this dication geometry as *displ*. We note that in the absence of intramolecular close **PD**$^+$ contacts, relatively close

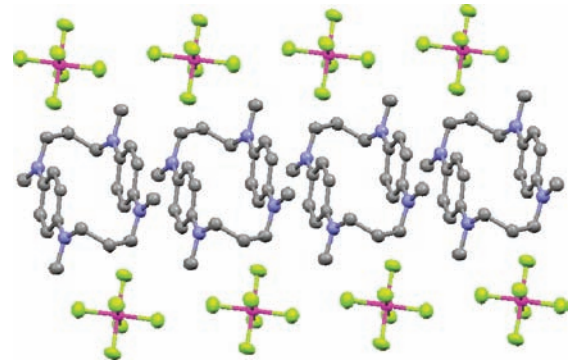

Figure 3. Crystal structure of **1(Me)**$^{2+}(SbF_6^-)_2$, showing the displacement of its **PD**$^+$ units and close contacts between nonbonded **PD**$^+$ units.

intermolecular ones were obtained for the dication units, although they have their **PD**$^+$ units displaced from each other.

1(iPr)$^{2+}$ has a crystal structure very different than that of **1(Me)**$^{2+}$ and **1(Et)**$^{2+}$, because its NCCC units are *aa*,*aa*, placing the **PD**$^+$ units as far apart as possible. The neutral compound is *ga*,*ga*,[1] so instead of the rings approaching each other upon electron removal as they do for the methyl- and ethyl-substituted compounds, they become slightly further apart for the branched-alkyl isopropyl-substituted compounds. Table 2 compares the X-ray structures in this series that lack intramolecular π-stacking. Although close intramolecular **PD**$^+$ ring contacts for **1(iPr)**$^{2+}$ are precluded by its *aa*,*aa* geometry, its crystals have intermolecular mean C_6 planes that are parallel and separated by only 2.94 Å, which is slightly shorter than the intramolecular mean plane distances of the *gg*,*gg* methyl and ethyl compounds. See Figure 4 for a drawing. The **PD**$^+$ planes are displaced from each other, but the closest CH,CH distances are 3.04 Å, which is below formal vdW contact distance, as is the closest distance between quaternary carbons, 3.12 Å. We note that the C_6 rings of **1(iPr)**$^{2+}$ are more distorted from planarity than any of the other **1(R)**$^{2+}$ structures. It is bent toward a boat geometry with $\sum|\angle CCCC| = 37.8°$, in the direction to allow closer approach of the C_6 rings. The two **1(Me)**$^{2+}$ structures in Table 1 have $\sum|\angle CCCC|$values of 17.5° and 21.4°, and the **1(Et)**$^{2+}$ structure 25.1°. In contrast, the displaced **PD**$^+$ unit **1(Me)**$^{2+}$ structure of Table 2 that also has relatively close intermolecular contacts but lacks the bulky branched alkyl substituents has the least distorted C_6 rings, $\sum|\angle CCCC| = 9.5°$.

Because **1(Me)**$^{2+}$ and **1(Et)**$^{2+}$ have singlet ground states, they show ^{1}H NMR spectra that narrow as the temperature is lowered because the tiny amount of triplet present, estimated at 1% in CD_3CN but shown to be sensitive to solvent, causes great

Table 2. Comparison of **1(R)**$^{2+}$ Structures Lacking Intramolecular π-Stacking

compd	**1(Me)**$^{2+}$$(SbF_6^-)_2$ *displ*	**iPr3C**$^{2+}$$(SbF_6^-)_2$ (plus unres. solvent)[d]
NCCC conformations	*gg*,*gg*	*aa*,*aa*
PD$^+$ conformations	*syn*,*syn*	*syn*,*syn*
NCCC twists, deg	±63.8, ±60.7	168.2, 168.2, 168.0, 168.0
d(N,N), Å	3.733	4.933, 4.965
d(C_q,C_q), Å	3.753[c]	5.284, 5.266[c]
d(CH,CH), Å	3.796, 3.806[d]	3.631, 3.634[d]
d(intramol C_6 planes), Å, or if not ||, their ∠, deg	3.295 Å	85.8°[e]
d(intermol. C_6 planes)	3.177	2.938
closest *d*(CH,CH), Å	3.325, 3.326	3.041, 3.041
NC twists,[a] deg	±8.2, ±15.3, ±13.7, ±11.7	−11.6, −4.1, −11.6, −4.1

[a] C=C−N−R twist, C=C′−N−CH_2 twist; average is N(lp),C(p) twist. [b] The solvent for this structure was too disordered to locate, and was omitted from the refinement. [c] Distance between pairs of quaternary ring carbons. [d] Distances between the closest ring carbons. [e] Intramolecular angle, deg., between the average C_6 planes in the two aryl rings.

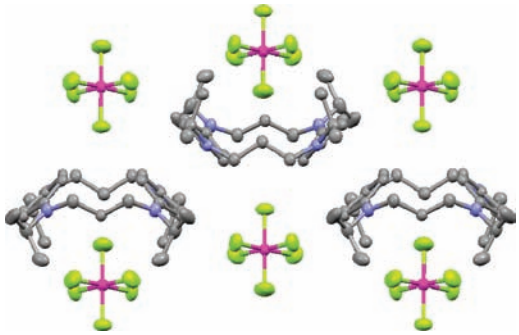

Figure 4. X-ray structure of **1(iPr)**$^{2+}$$(SbF_6^-)_2$ (disordered solvent not located, hydrogens not shown, and only the closer counterion is shown for the two peripheral dication units).

broadening.[1] The polar solvent mixture 2:1 CD_3OD/CD_3CN allows going to near −60 °C before the solvent freezes, where interconversion of the *gg*,*gg* conformations by CN rotation at the **PD**$^+$ rings has become slow on the NMR time scale, and reveals that three different *gg*,*gg* conformations are present in detectable amounts. The major conformation in solution has the **R** groups *syn* at both **PD**$^+$ units, abbreviated *syn*, so that the aromatic hydrogens appear as two 4H singlets having different chemical shifts. The conformation with the **R** groups *anti* at both **PD**$^+$ units, abbreviated *anti*, which was the major (or only) conformation found in crystals, has the aromatic hydrogens appear as two 4H AA′BB′ approximate doublets of doublets, separated by a $^3J_{HH}$ of about 9 and $^4J_{HH}$ of about 2 Hz, was also present. Finally, a conformation having the **R** groups *syn* at one **PD**$^+$ unit but *anti* at the other is also present, abbreviated *uns*, and shows eight different chemical shift aromatic CH AA′BB′ approximate doublets of doublets, some of which almost overlap. The substantial range of about 1.5 δ for the aromatic protons of the *uns* conformation is consistent with substantial cross-ring interactions, indicating that *uns*, as well as the *syn* and *anti* conformations found in the crystals, has ∠NCCC *gg*,*gg* and close approach of its **PD**$^+$ rings. Low temperature spectra for **1(Me)**$^{2+}$ appear in Figure 5 and **1(Et)**$^{2+}$ in Figure 6. The *uns* conformation is clearly present in smaller relative population for **1(Et)**$^{2+}$than it is for **1(Me)**$^{2+}$ and the spectra are distinctly narrower at all temperatures for **1(Et)**$^{2+}$, implying a smaller thermally accessible triplet content, which is consistent with the statistically significantly closer **PD**$^+$ units found in the X-ray structure. Integration of these spectra gave relative populations of **1(Me)**$^{2+}$ *syn*:*anti*:*uns* of 54:17:29 at −58 °C, and **1(Et)**$^{2+}$ *syn*:*anti*:*uns* of 68:20:12 at −60 °C.

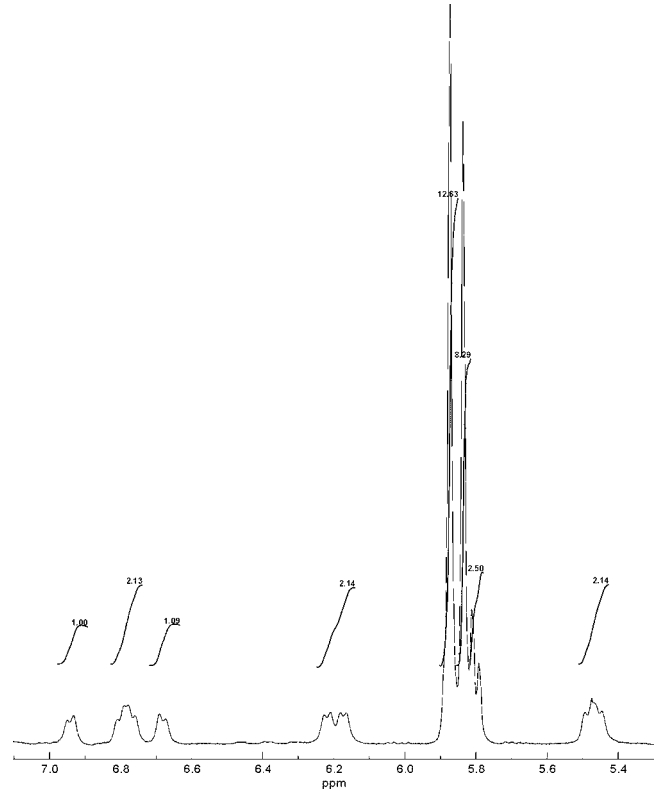

Figure 5. ^{1}H NMR spectra of **1(Me)**$^{2+}$$(PF_6^-)_2$ in CD_3OD/CD_3CN (2:1 v/v), recorded at −58 °C (at 500 MHz). The downfield *anti* 4H "doublet" overlaps almost completely with the downfield *syn* signal.

We note that the order of relative populations of solution conformations is significantly different with methyl and ethyl substituents, which is noteworthy for so small a structural change.

Discussion

Electron correlation is obviously important for these π-stacked open shell structures, so DFT methods that include electron correlation relatively inexpensively are indicated for doing calculations to understand the spectra of these compounds. However, B3LYP is exceptionally poor for π-stacking problems,[2] and **1(R)**$^{2+}$ proves to be no exception. B3LYP gets the

(2) Zhao, Y.; Truhlar, D. G. *Acc. Chem. Res.* **2008**, *41*, 157–167.

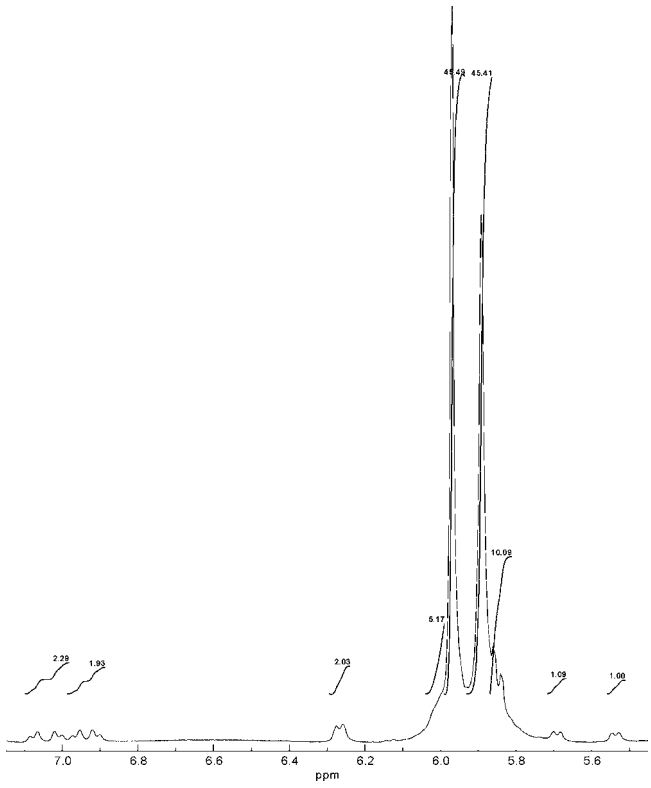

Figure 6. 500 MHz ^{1}H NMR spectra of **1(Et)**$^{2+}$(SbF_6^-)$_2$ in CD_3OD/CD_3CN (2:1 v/v), recorded at −60 °C (at 500 MHz). The downfield *anti* 4H "doublet" does not overlap with the downfield *syn* signal as completely as it does for **1(Me)**$^{2+}$·[SbF_6^-]$_2$.

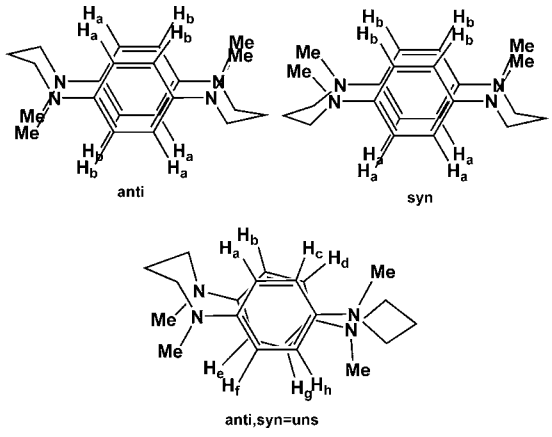

PD$^+$ rings in **1(Me)**$^{2+}$ to repel each other, as they do in the neutral compounds, so the *aa*,*aa* conformation is calculated to be the most stable, as it is for the neutral compound, the triplet states to be more stable than the singlet states, and the *gg*,*gg* conformations are calculated to have the rings separated by distances close to vdW contacts. Experimentally, the singlet states are significantly more stable than the triplets, and the *gg*,*gg* conformations are most stable, and the rings are significantly closer than vdW contact, so B3LYP calculations are nearly useless for understanding these compounds. Because the relative populations of three similar energy conformations are known experimentally for both **1(Me)**$^{2+}$ and **1(Et)**$^{2+}$, these compounds provide a rare opportunity to test methods of calculating these structures. Grimme has recently examined several methods and discussed the need for rather high level SCS-MP2 calculations with valence triple-ζ basis sets to properly reproduce the X-ray

Table 3. Summary of Relative Energies and Predicted Populations Obtained from Calculations[a] on Singlet **1(Me)**$^{2+}$, Compared with Populations Observed Experimentally

	LDA		M06-2X[b]		B3LYP[c]		NMR
config	rel E[d]	%	rel E[d]	%	rel E[d]	%	%
syn	0.00	61	0.00	65	0.00	41	54
anti	0.54	17	0.47	22	0.62	10	17
uns	1.02	22	1.28	13	0.52	49	29

[a] All calculations used a 6-311+G(d) basis set and an integration quadrature with 75 radial points (Euler−Maclarin) and 302 angular points (Lebedev). A finer grid, (99,302) verified convergence. [b] M06-2X is a hybrid meta functional developed by the Truhlar group[2] that shows better performance for π-stacking. [c] The relative amounts given are calculated at the −58 °C of the NMR experiment and consider only the three conformations shown. All three of these conformations are actually calculated to lie far too high in energy to be populated detectably using B3LYP. [d] Relative energies in kcal/mol.

Table 4. Summary of the Relative Energies and Predicted Populations Obtained from Calculations[a] on Singlet **1Et**$^{2+}$ with the Populations Observed Experimentally

	LDA		NMR
config	rel E[a]	%	%
syn	0.00	60	68
anti	0.42	22	20
uns	1.10	18	12

[a] Using a 6-311+G(d) basis set and an integration quadrature with 75 radial points (Euler−Maclaurin) and 302 angular points (Lebedev). The populations are calculated at the −60 °C temperature of the NMR experiment.

structures of the exceptionally strained [2.2]paracyclophane and its analogues.[3] Rather surprisingly, local density approximation, LDA, calculations using Dirac−Slater exchange[4] and parametrization no. 5 of the Vosko, Wilk, and Nusair correlation[5] do an absolutely remarkably good job of predicting the relative populations of conformations of these π-stacked diradical dications. Comparisons of the results of three calculation methods for **1(Me)**$^{2+}$ are shown in Table 3. There are a couple of important things about the table. First, due to the symmetry of the molecule, there are two different ways to form a *syn* conformation with the same energy. That is to say, it has a degeneracy (σ) of 2. The same is true for *anti*, whereas $\sigma = 8$ for *uns*. These numbers have been taken into account when calculating the relative populations using the fractional population, $f = \sigma(\exp(-\Delta E/RT)/[\sum\sigma(\exp(-\Delta E/RT)]$. Second, enthalpy corrections are not included in the energies because they are not necessary for these very similar conformations. LDA frequency calculations for the *syn*, *anti*, and *uns* conformations of **1(Me)**$^{2+}$ show that all are energy minima and give nearly identical enthalpy corrections at 298 K (330.757, 330.704, and 330.788 kcal/mol, respectively), which is below any reasonable expectation of error for such calculations.

The situation is slightly different for **1Et**$^{2+}$ because rotation of the ethyl along the C−N bond generates different rotamers. However, we expect the rotational barrier to be low; thus the lowest energy rotamer for each conformation is used to calculate the relative populations with the same degeneracies as **1(Me)**$^{2+}$.

(3) Grimme, S. *Chem.—Eur. J.* **2004**, *10*, 3423–3429.
(4) (a) Dirac, P. A. M. *Proc. Cambridge Philos. Soc.* **1930**, *26*, 376–385. (b) Slater, J. C. *The Self-Consistent Field for Molecules and Solids. Quantum Theory*; International Series in Pure and Applied Physics, Vol. 4; McGraw-Hill: New York, 1974;.
(5) Vosko, S. H.; Wilk, L.; Nusair, M. *Can. J. Phys* **1980**, *58*, 1200.

Table 5. Comparison of Calculated Geometries for **1(Me)$^{2+}$**[a]

	1(Me)$^{2+}$			
	syn	*anti*	*uns*	*displ*
∠NCCC, deg[b]	66.5, −67.4, 67.0, −68.2	69.3, −68.1, −69.3, 68.1	−55.2, −55.8, −58.3, 71.7	59.3 × 2, −59.3 × 2
d(NN), Å	2.963,2.953	2.968 × 2	2.857. 3.408	3.526 × 2
d(C_qC_q), Å	3.057,3.051	3.050 × 2	2.972,3.257	3.332 × 2
closer	3.028,3.025	3.093 × 2	3.159,3.279	2.996 × 2
d(CH,CH)	3.243,3.239	3.145 × 2	3.179,2.997	3.303 × 2
mean C_6 plane angle, deg	5.3	0	3.9	0
mean C_6 plane distance	not ||	3.039	not ||	2.895

[a] All optimized with 77 radial and 302 angular points. [b] ∠NCCC values are quoted for each NCCCN unit separately.

Table 6. Comparison of Calculated Geometries for **1(Et)$^{2+}$**[a]

	1(Et)$^{2+}$		
	syn	*anti*	*uns*[b]
∠NCCC, deg[c]	±61.2, ±61.8	±61.6, ±61.8	52.0, −67.8, 55.3, 54.7
d(NN), Å	2.823, 2.824	2.818, 2.819	2.741, 3.504
d(C_qC_q), Å	2.991, 2.992	2.980 × 2	2.950, 3.288
closer	2.966 × 2	3.052 × 2	3.035, 3.171
d(CH,CH)	3.218 × 2	3.105, 3.106	3.214, 3.299
mean C_6 plane angle, deg	6.3	0	2.9
mean C_6 plane distance	not ||	2.933	not ||

[a] All optimized with 77 radial and 302 angular points. [b] Unexpectedly, the conformation with the *N*-ethyl groups on the NCCCN group having the signs for its two NCCC units the same, like both NCCCN groups are for **1(Me)$^{2+}$**, the ethylated *uns* is calculated to be 0.5 kcal/mol more stable with the ethyl group methyls directed "inward", toward the $(CH_2)_3$ groups, than "outward", away from them, like all the ethyl groups of *anti* and *syn*. It is not clear why this is calculated to occur, but using the lowest energy calculated *uns* structure fits the NMR data better. [c] ∠NCCC values are quoted for each NCCCN unit separately.

Table 4 includes similar information as Table 3 for LDA calculations on **1Et^{2+}**.

The calculated geometrical information for **1(Me)$^{2+}$** are compared in Table 5, and that for **1(Et)$^{2+}$** is in Table 6.

Comparing with the X-ray structures, the calculated short intermolecular distances that are below vdW contact are calculated to be somewhat too small for the *anti* conformations, the ones for which the X-ray geometries are best, by 0.04 for N,N, 0.08 for C_q,C_q, and 0.10 and 0.06 for the shorter CH distances for **1(Me)$^{2+}$** and 0.02 for N,N, 0.03 for C_q,C_q, and 0.04 and 0.01 Å for the shorter CH,CH distances of **1(Et)$^{2+}$**. We note that the slightly smaller distances found by X-ray for **1(Et)$^{2+}$** than for **1(Me)$^{2+}$** are also present in these calculations.

The results of Tables 3−5 are especially surprising because there has been a general feeling in the community that counterion placement and solvent effects are crucial in predicting geometries for π-stacked radical ions since the suggestion by Miller and co-workers that counterion placement was crucial in allowing tetracyanoethylene radical anion (**TCNE$^-$**) to form the long bonded "pseudo-cyclobutanoid" conformations found in its crystals, apparently largely on the basis of B3LYP calculations.[6] Thus even when LDA calculations were applied to thiophene oligimer radical cation dimers by Sherlis and Marzari, they concluded that the gas-phase energy minimum obtained could not be correct because B3LYP and other methods obtained no minimum without the presence of counterions or solvent.[7] It is not obvious that electrostatics play the dominant role in the bonding between π-stacked radical ions, and our belief is mainly based on experimental evidence such as those in Kochi's work.[8] The most recent paper from the Kochi group (published after his death) concludes that counterion placement is a relatively minor factor for the dimers of substituted benzoquinone radical anions.[9] It is a pleasant surprise to find that gas-phase, no-counterion LDA calculations do so well for these compounds that have π-stacking enforced by their trimethylene bridges. Theoretically, LDA is only applicable to systems with slowly varying electron densities, to which most molecules do not belong. The justification of using LDA for molecules can only be its success in numerical applications, and that seems to be true here, as well as in some other neutral π-stacking systems.[10] On the other hand, Jung and Head-Gordon have emphasized the importance of dispersion interactions in determining the structures of $TCNE^-$ dimers.[11] It is well-known that LDA lacks proper account of dispersion interactions; it overbinds rare gas atom dimers[12] and give quite poor results for benzene dimers when dispersion corrections were applied.[13] Thus LDA may not be the best choice to be used in a theoretical debate. However, as a practical measure, LDA offers computational advantages over more sophisticated functionals and high-level quantum chemistry methods. We are currently doing more comparisons of experiments and calculations to test the general applicability of LDA in π-stacking systems.

Starting from the X-ray geometry of the displaced **PD$^+$** structure of **1(Me)$^{2+}$**$(SbF_6^-)_2$ in Table 2 (*displ*), an LDA optimization at the same level as those in Table 3 retained the *displ* structure and is 4.3 kcal/mol higher in energy than the

(6) (a) Nuvoa, J. J.; Lafuente, P.; Del Sesto, R. E.; Miller, J. S. *Angew. Chem., Int. Ed.* **2001**, *40*, 2540–2545. (b) Del Sesto, R. E.; Miller, J. S.; Novoa, J. J.; Lafuente, P. *Chem.—Eur. J.* **2002**, *8*, 4894–4908.
(7) Sherlis, D. A.; Marzari, N. *J. Phys. Chem. B* **2004**, *108*, 17791–17795.
(8) (a) Lü, J.-M.; Rosokha, S. V.; Kochi, J. K. *J. Am. Chem. Soc.* **2003**, *125*, 12161–12171. (b) Rosokha, S. V.; Kochi, J. K. *J. Am. Chem. Soc.* **2007**, *129*, 3583–3697. (c) Rosokha, S. V.; Lu, J.; Rosokha, T. Y.; Kochi, J. K. *Phys. Chem. Chem. Phys.* **2009**, *11*, 324–332.
(9) Rosokha, S. V.; Lu, J.; Rosokha, T. Y.; Kochi, J. K. *Phys. Chem. Chem. Phys.* **2009**, *11*, 324–332.
(10) Swart, M.; van der Wijst, T.; Guerra, C. F.; Bickelhaupt, F. M. *J. Mol. Model.* **2007**, *13*, 1245–1257.
(11) Jung, Y.; Head-Gordon, M. *Phys. Chem. Chem. Phys.* **2004**, *6*, 2008–2011.
(12) Kristyan, S.; Pulay, P. *Chem. Phys. Lett.* **1994**, *229*, 175–180.
(13) Meijer, E. J.; Sprik, M. *J. Chem. Phys.* **1996**, *105*, 8684–8689.

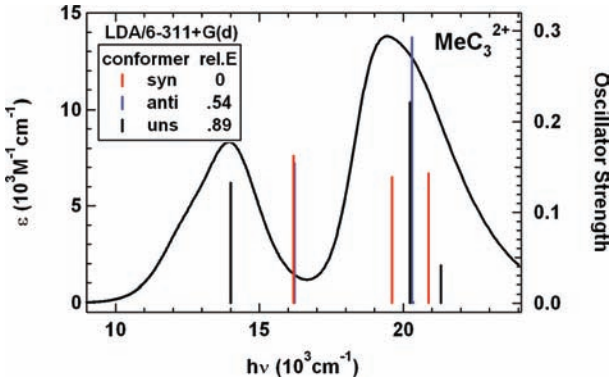

Figure 7. Optical spectrum of **1(Me)**$^{2+}$ at room temperature compared with stick spectra calculated for *syn*, *anti*, and *uns* conformations.

most stable *syn* geometry, suggesting that some kinetic reason is involved in obtaining this geometry for the dication unit when it is crystallized from an excess of the neutral compound, where monocation is expected to be the principal oxidation level present.

TD-LDA calculations of the optical spectra were carried out on the three conformations of **1(Me)**$^{2+}$ known to be present from the NMR spectra at low temperature and are compared with the room temperature optical spectra in Figure 7. The striking feature of the optical spectrum of **1(Me)**$^{2+}$ is that the single Class III mixed valence band vibrational progression with a maximum at 16,200 cm^{-1} that is observed for tetramethyl-**PD**$^{+}$ and at about 15,200 cm^{-1} and somewhat broadened for **1(Me)** monocation appears as two considerably broadened bands that still appear to contain traces of vibrational structure, at 13,900 and 19,300 cm^{-1} in the spectrum of **MeC$_3$**$^{2+}$. These calculations successfully predict two bands in this spectral region for **1(Me)**$^{2+}$ and predict the band maximum of the second band rather well (the second band maximum for the *anti* conformation and average of the two bands for the *syn* conformation is only about 800 cm^{-1} higher than the observed band maximum), but they underestimate the separation between the bands. The first band maximum for the *anti* and *syn* conformations are calculated to be 2200 cm^{-1} higher than the first band maximum. Although the unsymmetrical conformation first band is calculated to be close to the observed maximum, we suggest that the lump on the rise of the low energy band indicates that its calculated energy is high by a comparable amount higher to that of the *anti* and *syn*. The molecular orbitals (MOs) involved in these transitions are calculated to be those shown in Figure 8. As might be expected, the highest occupied MO (HOMO) for singlet **1(Me)**$^{2+}$ is the through-space bonding combination of the SOMO of the "monomeric" **PD**$^{+}$,[14] MO 95, and its antibonding combination is the LUMO, MO 96. The reason for the rather larger than observed calculated transition energy for this band might be the shorter than observed inter-**PD** distances obtained by the LDA calculation; we would expect this transition energy to be very sensitive to the distance between the **PD**$^{+}$ groups. The second band, at 19300 cm^{-1} is assigned as being from (HOMO-1), MO 94, to the virtual orbital. The **1(Me)**$^{2+}$ (HOMO-1) is the antisymmetric combination of the symmetric **TMPD**$^{+}$ MOs involved in the **TMPD**$^{+}$ lowest energy "filled" to SOMO (type A)[14] transition at 16 300 cm^{-1}, so it has been shifted to substantially higher energy by the inter-**PD**$^{+}$ interaction in **1(Me)**$^{2+}$. A transition from (HOMO-2), MO 93, to the *LUMO* is calculated to occur at almost the same energy (so it is not separated from the MO 94 in the drawing) but to have almost no intensity, because its node in the **PD**$^{+}$ system passes through the two CN bonds, so there is little overlap with the LUMO.

(14) Nelsen, S. F.; Weaver, M. N.; Telo, J. P.; Lucht, B. L.; Barlow, S. *J. Org. Chem.* **2005**, *70*, 9326–9333.

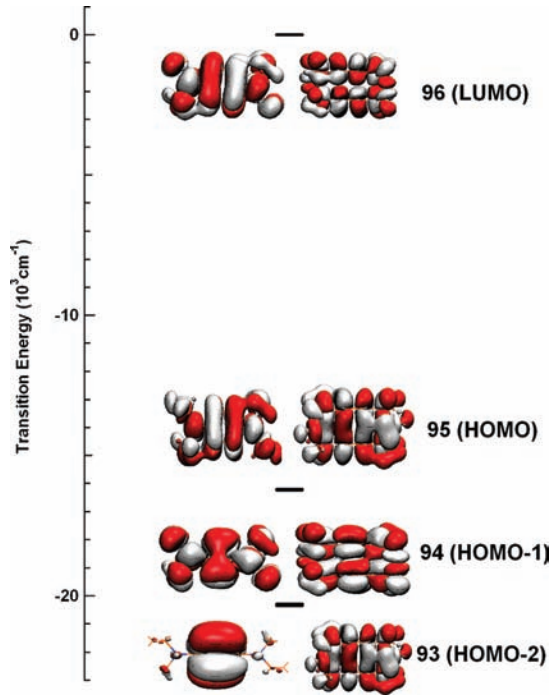

Figure 8. Molecular orbitals calculated to be involved in the transitions of *anti* **MeC$_3$**$^{2+}$.

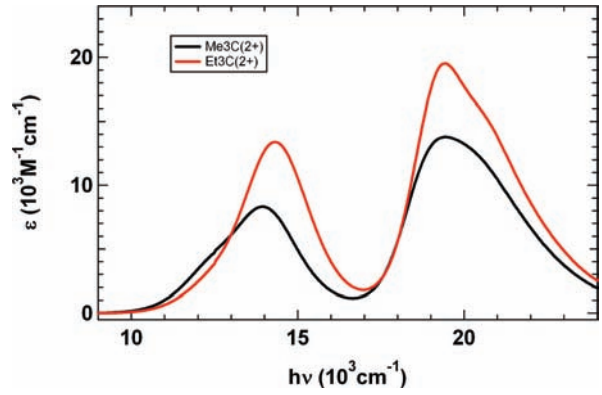

Figure 9. Comparison of the room temperature optical spectra of **1(Et)**$^{2+}$ (red) and **1(Me)**$^{2+}$ (black) in CH_2Cl_2.

The optical spectrum of **1(Et)**$^{2+}$ is much like that of **1(Me)**$^{2+}$ but, as shown in Figure 9, lacks the low energy bulge that the TD-LDA calculations attribute to the *uns* conformation, which the NMR studies demonstrate is present in much lower population relative to *syn* and *anti* for **1(Et)**$^{2+}$ than for **1(Me)**$^{2+}$, so this rather subtle feature of the optical spectra is also predicted by the TD-LDA calculations.

1(iPr)$^{2+}$ has a considerably different optical spectrum than the methyl- and ethyl-substiututed compounds and contains far more triplet (estimated at over 30 times as much as **1(Me)**$^{2+}$).[1] No NMR signal could be detected for it, presumably because of extensive broadening. The TD-LDA calculation for *ga,ga* **1(iPr)**$^{2+}$ is shown in Figure 10.

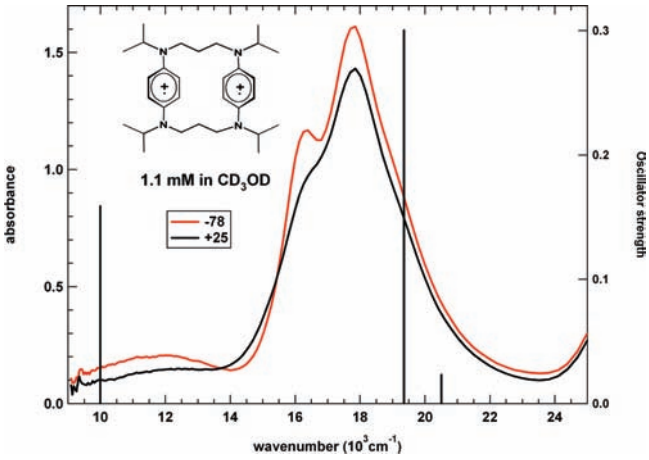

Figure 10. Comparison of experimental spectra for **1(iPr)**$^{2+}$ at 25 and −78 °C in methanol with the TD-LDA calculation.

The low energy band is calculated to be too low in energy, and the intensity relative to the high energy band is considerably overestimated.

Conclusions

Gas-phase LDA calculations without counterions successfully predict the order for relative populations of the three conformations of **1(Me)**$^{2+}$ and **1(Et)**$^{2+}$ that are observed by NMR and also that **1(Et)**$^{2+}$ has slightly closer **PD**$^{+}$ rings than **1(Me)**$^{2+}$, as is found by X-ray crystallography, and confirmed by the noticeable smaller broadening in its NMR at all temperatures, consistent with a smaller triplet content. Interestingly, both crystals of **1(R)**$^{2+}$ studied that do not have intramolecular close **PD**$^{+}$ distances because their trimethylene bridges are in geometries that prevent it have rather close intermolecular **PD**$^{+}$ approaches. TD-LDA calculations assign the optical spectra observed for **1(Me)**$^{2+}$ and **1(Et)**$^{2+}$ convincingly, demonstrating that the low energy band is caused by a transition between the occupied bonding and virtual antibonding combinations of the **TMPD**$^{+}$ SOMOs, whereas the higher energy band has its origin in an orbital of the same symmetry as that for the lowest energy band of **TMPD**$^{+}$ but is shifted about 3000 cm^{-1} higher in energy by the intramolecular interaction of the π systems in these dimeric systems.

Experimental Section

Materials. Synthesis of **1(Me)**, **1(Et)**, and **1(iPr)** was described previously.[1] Dication diradical salts **1(Me)**$^{2+}$(X^{-})$_2$, **1(Et)**$^{2+}$(X^{-})$_2$, and **1(iPr)**$^{2+}$(X^{-})$_2$ were prepared by oxidation of the corresponding paracyclophanes **1(R)** with stochiometric (1:2) amounts of corresponding nitrosonium salts $NO^{+}PF_6^{-}$, $NO^{+}SbF_6^{-}$, or [N(4-$C_6H_4B_r)_3$]$^{+}SbCl_6^{-}$ in dichloromethane with a small amount of acetonitrile present, which was added in order to increase the solubility of the dication salt. The resulting purple solution of dication diradical salt was precipitated by adding excess hexanes. When [N(4-$C_6H_4B_r)_3$]$^{+}SbCl_6^{-}$ was used as oxidant, the neutral product amine was washed away with small amount of cold dichloromethane several times. Single crystals of the dication diradical salts, **1(Me)**$^{2+}$($SbCl_6^{-}$)$_2$, **1(Et)**$^{2+}$($SbCl_6^{-}$)$_2$, and **1(iPr)** $^{2+}$(SbF_6^{-})$_2$ were prepared by dissolving the diradical dication salts in dichloromethane with small amount of acetonitrile, and the resulting clear solutions were overlaid with a small amount of the mixture of dichloromethane and hexanes, which was again overlaid with hexane. The solvent mixture was kept in the refrigerator for 1 week. The conformation of the *displ* **1(Me)**$^{2+}$(SbF_6^{-})$_2$ crystal was prepared by dissolving an excess amount of neutral **1(Me)** in dichloromethane and oxidizing with a small amount of oxidant $NO^{+}SbF_6^{-}$, producing the dark blue colored monocation solution. Dinitrogen was bubbled through the solution to remove the nitric oxide (NO) gas, the solution was layered with hexane, and the solid formed after several days in a refrigerator.

Optical Spectral Measurements. Optical spectra were acquired on a Varian Cary 50 scan UV−vis spectrometer (200−1100 nm) using capped quartz cuvettes with side arms. Low temperature measurements were performed by cooling to the corresponding temperature of solution in a Dewar under inert atmosphere and rapid scanning of the cold sample under survey mode (baseline correction was measured similarly using pure solvent).

Low Temperature NMR Measurements. 1(Me)$^{2+}$(PF_6^{-})$_2$ in 2:1 CD_3OD/CD_3CN at −58 °C. ^{1}H NMR aromatic H shifts (δ): *uns* 6.93, ∼6.79 (2H), 6.69, 6.21, 6.18, ∼5.47 (2H); *syn* 5.87, 5.84; *anti* (∼5.87, overlaps with *syn*), 5.80.

1(Et)$^{2+}$(PF_6^{-})$_2$ in 2:1 CD_3OD/CD_3CN at −60 °C. ^{1}H NMR aromatic H shifts (δ): *uns* 7.07, 7.02, 6.95, 6.92, ∼6.26 (2H), 5.70, 5.54; *syn* 5.97, 5.89; *anti* ∼6.02 (overlaps badly with *syn*), 5.85.

Calculations. The local density approximation (LDA), with Dirac−Slater exchange[4] and parametrization no. 5 of the Vosko−Wilk−Nusair correlation,[5] was used for the ground state geometry optimization. The LDA functional is known for its tendency of overbinding, i.e., giving excessive binding energies.[15] Nonetheless, it was found to describe $\pi-\pi$ stacking reasonably well for both neutral[16] and charged[17] monomers. All our calculations were performed with the Q-Chem software package, version 3.2.[18] Optical spectra were calculated with time-dependent density functional theory,[19,20] again using the LDA functional.

Acknowledgment. S.F.N. thanks the National Science foundation for support under CHE-0647719. Q.W. is supported by the U.S. Department of Energy, Office of Basic Energy Sciences, under Contract No. DE-AC02-98CH10886.

Supporting Information Available: Optical spectrum of **1(Me)**$^{2+}$($SbCl_6^{-}$)$_2$ in 2:1 CH_3OH/CH_2Cl_2 as a function of temperature and of the solid at room temperature, ORTEP drawing of the unreported crystal structure of **1(Me)**$^{2+}$-($SbCl_6^{-}$)$_2$·2($ClCH_2$)$_2$, ^{1}H NMR spectra of **1(Me)**$^{2+}$ and **1(Et)**$^{2+}$ and ^{13}C NMR of **1(Me)**$^{2+}$ in 2:1 CD_3OD/CD_3CN, structural reports on the four X-ray structures, *xyz* coordinates of the LDA-optimized structures, TDLDA output for **1(Me)**$^{2+}$, and complete ref 18. This material is available free of charge via the Internet at http://pubs.acs.org.

JA100322K

(15) Kohn, W.; Becke, A. D.; Parr, R. G. *J. Phys. Chem.* **1996**, *100*, 12974–12980.
(16) Swart, M.; van der Wijst, T.; Guerra, C. F.; Bickelhaupt, F. M. *J. Mol. Model.* **2007**, *13*, 1245–1257.
(17) Scherlis, D. A.; Marzari, N. *J. Phys. Chem. B* **2004**, *108*, 17791–17795.
(18) Shao, Y.; et al. *Phys. Chem. Chem. Phys.* **2006**, *8*, 3172–3191.
(19) Runge, E.; Gross, E. K. U. *Phys. Rev. Lett.* **1984**, *52*, 997–1000.
(20) Casida, M. E. In *Recent Advances in Density Functional Methods, Part I*; Chong, D. P., Ed.; World Scientific: Singapore, 1995.